

BARBERPOLE PHASING AND FLANGING ILLUSIONS

Fabián Esqueda*, Vesa Välimäki

Aalto University
Dept. of Signal Processing and Acoustics
Espoo, Finland
fabian.esqueda@aalto.fi
vesa.valimaki@aalto.fi

Julian Parker

Native Instruments GmbH
Berlin, Germany
julian.parker@native-instruments.de

ABSTRACT

Various ways to implement infinitely rising or falling spectral notches, also known as the barberpole phaser and flanging illusions, are described and studied. The first method is inspired by the Shepard-Risset illusion, and is based on a series of several cascaded notch filters moving in frequency one octave apart from each other. The second method, called a synchronized dual flanger, realizes the desired effect in an innovative and economic way using two cascaded time-varying comb filters and cross-fading between them. The third method is based on the use of single-sideband modulation, also known as frequency shifting. The proposed techniques effectively reproduce the illusion of endlessly moving spectral notches, particularly at slow modulation speeds and for input signals with a rich frequency spectrum. These effects can be programmed in real time and implemented as part of a digital audio processing system.

1. INTRODUCTION

Shepard introduced in the 1960s the infinitely ascending chromatic scale, which was produced with additive synthesis [1, 2]. Risset expanded this idea by designing a continuously rising and falling sweep [3, 4]. The spectrum of two instances of the Shepard tone are shown in Figure 1. It is seen that the sinusoidal components are equally spaced in the logarithmic frequency scale, as each component is one octave higher than the previous one. A bell-shaped spectral envelope function takes care of the fade-in and fade-out of harmonic components. In addition to Shepard-Risset tones, other auditory illusions have been discovered, including binaural paradoxes [5] and rhythms which appear to be gaining speed in a never-ending manner [4, 6]. This paper discusses impossible-sounding phasing and flanging effects inspired by the Shepard-Risset tones.

Flanging is a delay-based audio effect which generates a series of sweeping notches on the spectrum of a signal [7, 8, 9, 10]. Historically, analog flanging was achieved by mixing the output of two tape machines and varying their speed by applying pressure on the flanges—hence the effect’s name [7, 9, 10]. Adding a signal with a delayed version of itself results in a comb filtering effect, introducing periodic notches in the output spectrum. As the length of the delay changes over time, the number of notches and their position also changes, producing the effect’s characteristic swooshing or “jet aircraft” sound [7, 9]. Wanderley and Depalle

[11, 12] have found that a flanging effect is also produced when a musician moves in front of the microphone while playing, as the time delay between the direct sound and its reflection from the floor is varied.

Phasing was introduced in effect pedals as a simulation of the flanging effect, which originally required the use of open-reel tape machines [8]. Phasing is implemented by processing the input signal with a series of first- or second-order allpass filters and then adding this processed signal to the original [13, 14, 15]. Each allpass filter then generates one spectral notch. When the allpass filter parameters are slowly modulated, the notches move up and down in frequency, as in the flanging effect. The number and distribution of the notches are the main differences between phasing and flanging, which can sometimes sound quite similar.

Bode developed a barberpole phaser in which the spectral notches move endlessly in one direction in frequency [16]. The name ‘barberpole’ stems from a rotating cylindrical sign, usually white with a red stripe going around it, which have been traditionally used in front of barber shops in England and in the US. As the pole rotates, a visual illusion of the red stripe climbing up endlessly along the pole is observed, although the pattern is actually

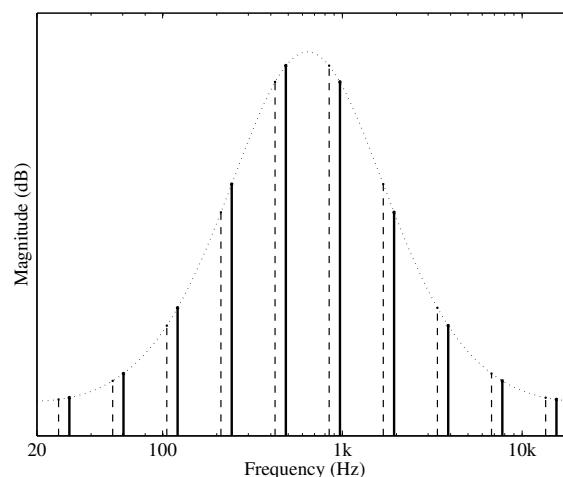


Figure 1: *Spectrum of a Shepard tone with 10 harmonics (solid lines), spaced one octave apart, and a raised-cosine spectral envelope (dotted line) [1]. The dashed lines show the harmonics a short time earlier.*

* The work of Fabián Esqueda is supported by the CIMO Centre for International Mobility and the Aalto ELEC Doctoral School.

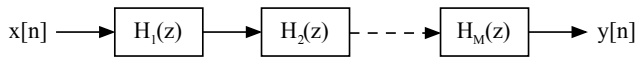


Figure 2: Block diagram for the proposed network of M time-varying notch filters $H_m(z)$ for $m = 1, 2, 3, \dots, M$. The center frequencies of these filters are situated at one-octave intervals.

stationary. Barberpole phasing and flanging effects are currently available in some audio software, but it is not known to us how they are implemented [17, 18].

Related recent work has focused on virtual analog models of vintage flanger and phaser circuits, such as the digital modeling of the nonlinear behavior caused by the use of operational transconductance amplifiers [19] and bucket-brigade devices [20]. Eichas et al. [21] have presented a detailed virtual analog model of a famous phaser. Furthermore, some research has focused on understanding how flanging, phasing, and other audio effects processing is recognized by humans [22] or by the computer [23].

In this paper we investigate ways to implement barberpole phasing and flanging effects. The inspiration for this comes from inverting the Shepard-Risset tone, i.e. replacing the spectral peaks with notches, to create a new impossible audio effect. In the end, we found that there are at least three different principles to obtain this effect. This paper is organized as follows. Section 2 discusses the basic cascaded notch filter technique to simulate the barberpole phasing effect. Section 3 introduces a novel flanging method using a pair of delay lines. Section 4 describes a third method, derived from that of Bode, which has its roots in single-sideband modulation. Finally, Section 5 provides some concluding remarks.

2. CASCADED TIME-VARYING NOTCH FILTERS

The illusion of endless rising or falling sweeping notches, similar to that of the phasing effect, can be achieved using a network of cascaded time-varying notch filters (see Figure 2). To do so, we follow the design of the Shepard tone and place the center frequencies of the filters at one-octave intervals. This design choice translates into notches uniformly distributed along the logarithmic frequency axis. The amount of attenuation caused by each filter is determined using an inverted version of the raised-cosine envelope originally proposed by Shepard [1] (see Figure 1).

Considering the case of a rising notch sweep, as the center frequencies of the filters move up the spectrum, notches approaching the Nyquist limit (f_N) will gradually disappear. Similarly, notches coming from the low end of the spectrum will increase in depth as they reach the middle frequencies. Since the one-octave interval between notches is preserved at every time step, the center frequencies of the filters will eventually reach twice their initial value. At this point, we say the system has completed one full cycle. If the filter parameters are continuously reset one time step before the system completes a cycle, the illusion of an infinite filter sweep is generated. Therefore, to implement the illusion we only need to derive the center frequencies and their respective gain values for a single cycle. These parameters can then be stored in a table and read indefinitely during implementation.

To compute the necessary initial parameters, we begin by defining a system of M cascaded notch filters and denote the repetition rate of the effect, in Hz, by ρ . The total number of center

frequencies (denoted by K) each filter will go through before it completes a full cycle is the same for every filter and is determined by

$$K = \lfloor F_s / \rho \rfloor, \quad (1)$$

where F_s is the sampling rate of the system. The k^{th} center frequency for the m^{th} filter can then be computed from

$$f_c(m, k) = f_0 2^{\lfloor K(m-1) + k - 1 \rfloor / K} \quad (2)$$

for $k = 1, 2, 3, \dots, K$ and $m = 1, 2, 3, \dots, M$. The parameter f_0 is the center frequency of the first filter at the beginning of a cycle. Next, the k^{th} center gain of the m^{th} filter is defined as

$$L_c(m, k) = L_{\min} + \frac{(L_{\max} - L_{\min})(1 - \cos[\theta(m, k)])}{2}, \quad (3)$$

where L_{\min} and L_{\max} are the minimum and maximum attenuation levels in dB, respectively, and $L_{\max} < L_{\min} < 0$. The function θ is defined as

$$\theta(m, k) = 2\pi \frac{(m-1)K + k - 1}{MK}. \quad (4)$$

In summary, we must implement M notches that sweep uniformly throughout K frequencies, each with its own attenuation level. In order to achieve this amount of control for each filter, we can use a *parametric equalizer* (EQ) filter structure [24]. This type of second-order IIR filter is commonly used in graphic equalizers, since it allows users to increase (boost) or reduce (cut) the gain of a specific frequency band.

The z-domain transfer function for the cutting case of the parametric equalizer filter is given by

$$H(z) = \frac{\left(\frac{1+G\beta}{1+\beta}\right) - 2\left(\frac{\cos\left(\frac{2\pi f_c}{F_s}\right)}{1+\beta}\right)z^{-1} + \left(\frac{1-G\beta}{1+\beta}\right)z^{-2}}{1 - 2\left(\frac{\cos\left(\frac{2\pi f_c}{F_s}\right)}{1+\beta}\right)z^{-1} + \left(\frac{1-\beta}{1+\beta}\right)z^{-2}}, \quad (5)$$

where G is the scalar gain at the center frequency f_c (i.e. $10^{L_c/20}$) and β is defined as

$$\beta = \sqrt{\frac{G_B^2 - 1}{G^2 - G_B^2}} \tan\left(\frac{\Delta\omega}{2}\right), \quad (6)$$

where $\Delta\omega$ is the width of the filter at gain level G_B [24]. Figure 3 illustrates the relationship between these three parameters for a filter with arbitrary center frequency f Hz.

Now, the definition of $\Delta\omega$ is rather ambiguous in this case. It is generally taken to be the width of the filter 3 dB below the reference level (i.e. $G_B^2 = 1/2$). In our case, since notches near DC and f_N may not reach this level of attenuation, this particular definition is inadequate. For this reason, we instead define the filter bandwidths in terms of their Q factor

$$Q = \frac{2\pi f_c}{\Delta\omega F_s} \Leftrightarrow \Delta\omega = \frac{2\pi f_c}{Q F_s}. \quad (7)$$

Maintaining a constant Q for every filter, rather than a constant $\Delta\omega$, will ensure the notches are equally wide on the logarithmic axis. Otherwise, notches near DC would be much wider than those near f_N . Finally, we define G_B^2 to be arithmetic mean between a reference gain of 1 and G , yielding

$$G_B^2 = \frac{1 + G^2}{2}. \quad (8)$$

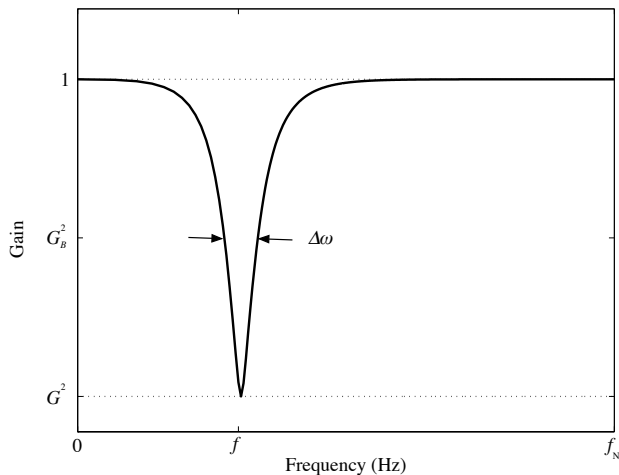


Figure 3: General form of the magnitude response of the parametric EQ filter in cut mode.

Figure 4 shows the magnitude response of the proposed system at its initial state. This implementation was realized with parameters $M = 10$, $\rho = 0.1$ Hz, $f_0 = 20$ Hz, $Q = 15$, $L_{\max} = -20$ dB and $L_{\min} = -3$ dB. A sampling rate $F_s = 44.1$ kHz was used for this and the rest of the examples in this paper. As we can see from the spectrum, the envelope of the notches resembles an inverted version of its Figure 1 counterpart. As expected, keeping the value of Q constant produces a fairly uniform notch distribution.

Figure 5 shows the spectrogram of a 30-second simulation of the barberpole illusion with the same parameters as in Figure 4 and white noise as the input signal. For this spectrogram and all those presented in this paper, a 1024-sample Chebyshev window with 100 dB of sidelobe attenuation, along with 512 samples of overlap were used. To increase image resolution at low frequencies, this particular signal was oversampled by a factor 10. The points in time where each cycle begins are marked with the three markers on top of the figure. Overall, in Figure 5 we can appreciate how, as

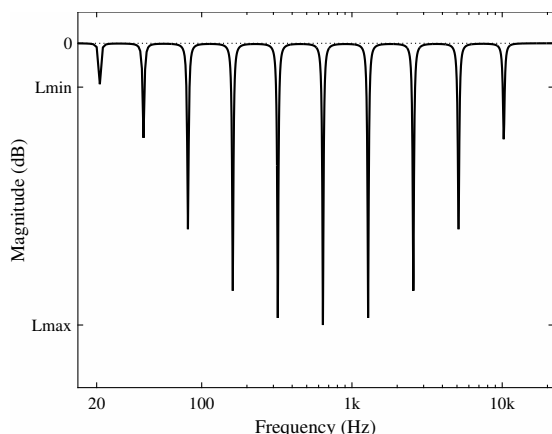


Figure 4: Magnitude response of a network of 10 cascaded parametric notch filters. The gain (attenuation) at each center frequency is determined by the raised-cosine envelope.

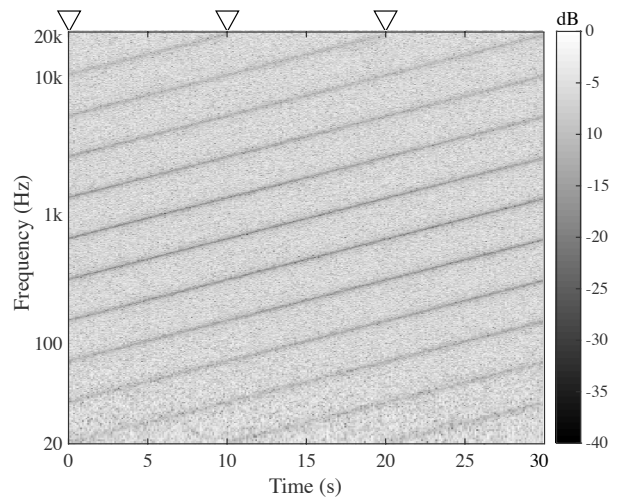


Figure 5: Spectrogram of a barberpole phaser illusion implemented using white noise filtered with $M = 10$ cascaded time-varying notch filters and $\rho = 0.1$. Starting points of the cycles are indicated with triangles.

the notches increase in frequency and approach the Nyquist limit, new ones begin to appear. Additionally, notches around the lower and upper ends of the spectrogram are clearly less dark, which translates into less attenuation. This system implementation requires f_0 and M to be chosen appropriately in order to ensure the last filter in the chain ends as close to the Nyquist limit as possible.

When implementing this illusion using a software routine, one additional consideration must be made. Once any given filter m reaches its K^{th} center frequency, it must reset to $k = 1$ at its next step. However, at this first time step of the new cycle the EQ filter requires the state variables of the previous filter $m - 1$ to correctly compute the output [25]. Therefore, the two final outputs and values of the delay state variables of each filter, which occur when $k = K - 1$ and $k = K$, must be passed on to the next filter. Failing to do so will introduce transients at the output of the network which will translate to audible clicks at the end of every cycle [25]. This would reveal the cyclic nature of the system and break the illusion.

Overall, this implementation of the barberpole phaser illusion works best for input signals with a dense and nearly flat magnitude spectrum, e.g. pink noise or noisy drum loops. Additionally, its parameters must be tuned differently for each input type. In terms of suitable values for ρ , numerous tests revealed that the illusion works best for values below 0.3 Hz. At higher rates, the cyclic nature of the design is also revealed and the illusion fails. This issue is also inherent to both the Shepard scale and the Shepard-Risset glissando which only work at slow playback rates.

Sound examples for this section can be found online at the accompanying website¹.

¹<http://research.spa.aalto.fi/publications/papers/dafx15-barberpole>

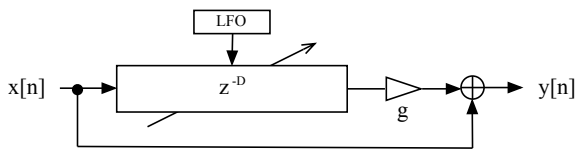


Figure 6: Block diagram of a basic digital flanger effect.

3. SYNCHRONIZED DUAL FLANGER

In the barberpole phasing approach discussed in the previous section, the number of notches remains constant throughout every cycle. This behavior is different to that of flanging, where the number of notches, along with their position, varies over time.

A barberpole version of the flanger effect can be implemented following the typical structure of a flanger in the digital domain, shown in Figure 6. In this system, the input is delayed by D samples, scaled by a gain factor g that controls the depth of the effect, and combined with the original signal. The length of the delay line is modulated by a sinusoidal or triangular low-frequency oscillator (LFO). Typical LFO rate values range between 0-3 Hz, while the maximum delay introduced by the delay line can be of up to 15 ms [9]. As the length of the delay line oscillates over time, the number of notches introduced and their position along the spectrum changes.

To implement the barberpole illusion, we first need to ensure the displacement of the notches is unidirectional. One possible solution is to use a sawtooth waveform for the LFO, which would ensure the length of the delay line is reset after every cycle. A trivial sawtooth LFO $s(n)$ can be synthesized for this purpose using a modulo counter [26]

$$s(n) = (D_{\max} - D_{\min})[(n\Delta) \bmod 1] + D_{\min}, \quad (9)$$

where n is the time step index, D_{\min} and D_{\max} are the minimum and maximum delay lengths (in samples), respectively, and $\Delta = \rho/F_s$ is the phase increment. As before, ρ is the rate of the effect. Since this waveform resembles an ascending ramp, the length of the delay line will gradually increase until it reaches D_{\max} . In the frequency domain this represents an increasing density of notches that move towards the lower end of the spectrum as they distribute themselves uniformly along the linear frequency axis. This effect is perceived as a descending filter sweep, contrary to the ascending nature of the LFO. To implement the effect in the opposite direction we just need to flip $s(n)$ horizontally, i.e. $s'(n) = (D_{\max} + D_{\min}) - s(n)$.

The abrupt transition from the maximum to the minimum delay lengths and vice versa can be described as a “hard reset” of

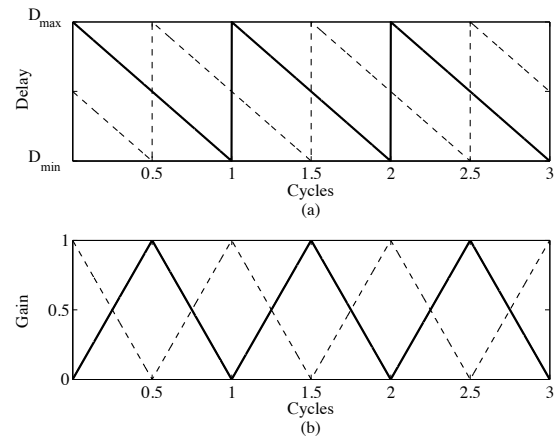


Figure 8: Waveforms for three cycles of (a) delay-line length controls LFO 1 (solid line) and LFO 3 (dashed line) and (b) gain controls g_1 (solid line) and g_2 (dashed line) of the synchronized dual flanger for the ascending flanger case, showing the 90° phase offset between pairs of oscillators. Cf. Figure 7.

the delay lines. This reset will generate a sudden change in the frequency content of the output signal that does not support the illusion of an infinitely ascending/descending sweep. To fix this issue the design can be extended to incorporate a second delay line at the output of the first one and use cross-fading to switch between them. The second delay line will have the same characteristics as the first one but its instantaneous length will be controlled by a 90° shifted version of the modulating LFO.

Figure 7 shows the block diagram of the proposed system. Two new LFOs (LFO 2 and LFO 4) have been added in order to modulate the gain blocks at the output of each delay line. The basic concept behind this design is to avoid the hard resets by switching between delay lines as they approach their maximum/minimum delay length. Triangular LFOs with a rate of ρ Hz can be used, for example, to implement a linear cross-fade. These new oscillators must be synchronized with the delay line modulators. Therefore, LFO 4 should also have a 90° phase shift in relation to LFO 2. Figure 8 shows the waveforms for three cycles of the four LFOs suggested for the design (ascending flanging case).

In order to make the notches travel smoothly in frequency the design can be expanded to incorporate fractional delay filters [27, 28], since modulation of the delay lengths will most likely require fractional delay lengths. Naïve implementations usually resort to rounding off these values, making the notches sweep in a step-like manner and introducing the well-known “zipper noise”.

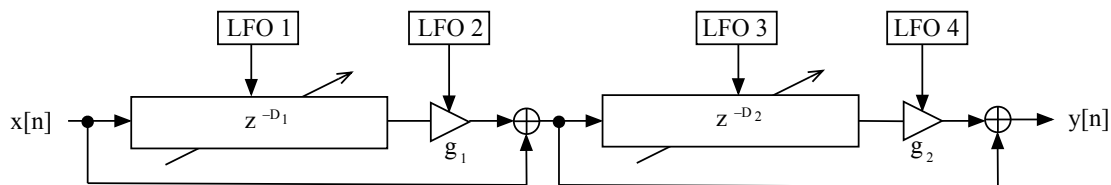


Figure 7: Block diagram of the proposed synchronized dual flanger system.

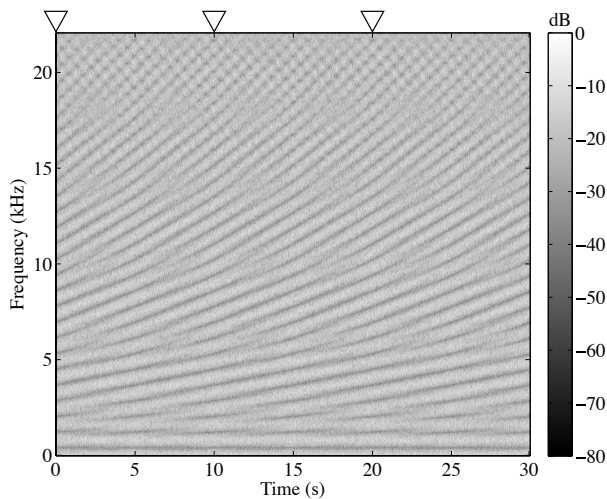


Figure 9: Spectrogram of white noise processed by the system described by Figure 7 and parameters $\rho = 0.1$ Hz, $D_{\max} = 66$ and $D_{\min} = 44$. The triangular markers atop the spectrogram indicate the points where the first delay line begins its cycle.

Figure 9 shows the spectrogram for a 30-second simulation of the effect using white noise as an input. For this example, the system parameters were set as $\rho = 0.1$ Hz, $D_{\max} = 66$ and $D_{\min} = 44$. Additionally, a third-order Lagrangian fractional delay filter was used to accommodate fractional delay lengths. As we can see from the spectrogram, the two flangers cross-fade over time and generate the illusion of a continuous sweep. The blurred portions on the spectrum represent the points where the two flangers meet. At high frequencies, the spectrogram shows the notch sweep is not as uniform as at low frequencies. This can be attributed to the lowpass response of the fractional delay interpolator and can be minimized using a higher order filter. Ideally, D_{\min} should be higher than half the value of D_{\max} . Otherwise, it becomes difficult to hide the hard resets and the illusion is broken. As before, this effect also works best at low rates.

Overall, this implementation can be heard on virtually any input signal. This can be attributed to the larger number of notches that can be easily achieved with considerably fewer operations per sample compared to the approach discussed in Section 2. However, the effect is still clearly more dramatic on signals with a relatively dense spectrum e.g. distorted guitars or drum loops. A real-time implementation of this effect can be easily achieved using circular buffers.

4. SINGLE-SIDEBAND MODULATION

A commonly known historical technique of producing barberpole-like phasing or flanging effects is to employ single-sideband (SSB) modulation, also known as frequency shifting. This technique was first described by Harald Bode [16]. The modulated signal is mixed with the un-modulated signal, producing notches in the combined spectrum which move at a rate dictated by the amount of frequency-shift applied. Feedback may be applied around this structure to strengthen the effect.

This effect initially seems counter-intuitive, as it contradicts our usual experience of combining two identical waveforms with

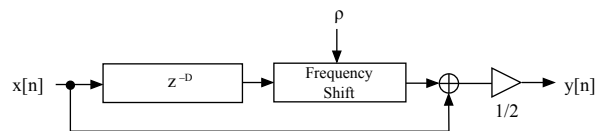


Figure 10: Block diagram showing generalized SSB-modulation based barberpole effect, capable of producing linearly spaced moving notches.

differing frequencies. Given an ideal frequency shifter operating on a sinusoid, with the frequency shifted sinusoid being mixed equally with the original sinusoid, we can write an expression describing the combination as a single sinusoid with time-varying amplitude and phase-shift:

$$\sin(\omega t) + \sin(\omega t + \omega_o t) = A(t) \sin[\omega t + \phi(t)], \quad (10)$$

where ω gives the angular frequency of the sinusoid, ω_o gives the amount of frequency shift, and t denotes time. $A(t)$ and $\phi(t)$ give the amplitude and phase of the combined waveform. With some manipulation and application of trigonometric identities, we can write an expression for the amplitude as:

$$A(t) = \sqrt{2 + 2 \cos(\omega_o t)}. \quad (11)$$

This expression seems to confirm our initial intuition, that combining two signals separated by a constant frequency offset should produce frequency independent beating. This is not consistent with the effect described by Bode and others. However, if a time delay between the shifted and un-shifted signals is added, the result is quite different. Given a time delay of τ , we have

$$\sin(\omega t) + \sin[(\omega + \omega_o)(t - \tau)] = A(t) \sin[\omega t + \phi(t)]. \quad (12)$$

Solving for A again, the following is produced:

$$A(t) = \sqrt{2 + 2 \cos(\omega_o t - \omega_o \tau - \omega \tau)}. \quad (13)$$

The addition of the time delay means that the phase of the amplitude variation with time for a particular frequency is offset depending on the frequency. If we assume linearity of the frequency shifter and delay, we can extend this result to an arbitrary input signal. Equation (13) then describes a set of notches in the frequency response of system, spread linearly over the frequency range and moving constantly in either the positive or negative frequency direction over time. The number of notches is related to the time delay, τ , and the rate and direction of movement is set by the frequency shift amount, ω_o .

The system described by Bode does not contain an explicit delay element. However, it relies on a ‘dome filter’—a parallel system of two chains of allpass filters with a relative phase delay difference of $\frac{\pi}{2}$. The allpass filter chains themselves introduce some (frequency-dependent) delay to the signal, therefore no additional delay element is needed to produce the effect.

Given the knowledge gained so far, we can design a generalised SSB-modulation based barberpole flanging effect with the structure described in Figure 10, where the rate (in Hz) and direction are controlled by $\rho = \omega_o f_s / 2\pi$. The length of the delay line $D = \tau f_s$ is related to the number of notches M by $M = D/2$.

In our generalised system, the design of the frequency shifter block is assumed to be based on the common method of quadrature

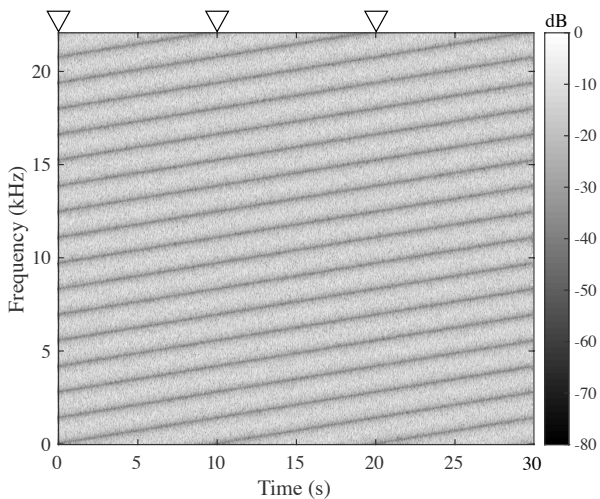


Figure 11: Spectrogram of white noise processed by the structure given in Figure 10. The delay is 32 samples, and the amount of frequency shift is 0.1 Hz. The markers on top indicate when the system starts a new cycle.

modulation of the real and imaginary parts of the analytic signal [29]. The analytic signal is produced via applying a Hilbert transform, which can be implemented in a variety of ways—as an FIR [30, 31] or IIR filter [32], as a digital version of the ‘dome-filter’ approach [33] taken by Bode, or via the use of an FFT. In this work we use the Matlab implementation of the Hilbert transform, which is based on the FFT.

The output of the system of Figure 10 when used to process an input of white noise is shown in Figure 11. The structure produces an interesting barberpole phasing effect, but does not convincingly produce the illusion of circularity given by the Shepard-Risset glissando. For this, octave distribution of the notches is necessary.

4.1. Warping the distribution of notches

Referring again to (13), we can see that to vary the spacing of the notches it is necessary to make the time delay, τ dependent on the frequency, ω . This can be achieved by replacing the delay line in the structure given in Figure 10 with a spectral delay [34], which can be implemented using a chain of first-order allpass filters, given by

$$A^D(z) = \left(\frac{a + z^{-1}}{1 + az^{-1}} \right)^D, \quad (14)$$

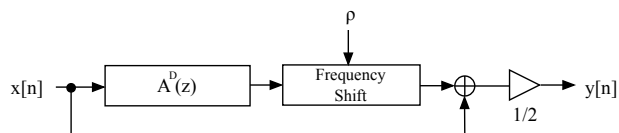


Figure 12: Block diagram showing SSB-modulation based barberpole effect using a spectral delay filter, capable of producing warped distribution of notches.

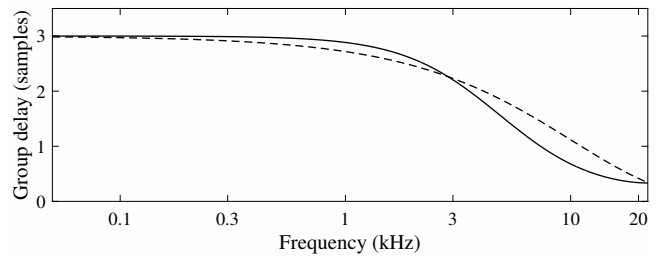


Figure 13: Desired group delay $3 \cdot 2^{-\omega}$ of the spectral delay filter (dashed line) and its approximation using a first-order allpass filter with $a = -0.5$ (solid line).

where a is the allpass filter coefficient and D is the number of stages. Spectral delay filters have been previously used for example for spring reverb emulation [35, 36] and for modeling the Leslie effect in Hammond organ synthesis [37].

The block diagram for the expanded configuration is shown in Figure 12. As in the linearly distributed case, the number of notches produced by this structure is given by $M = D/2$. The group delay of a first-order allpass filter is given by [34]

$$\tau_g(\omega) = \frac{1 - a^2}{1 + 2a \cos \omega + a^2}. \quad (15)$$

In order to achieve the ideal octave spacing of notches specified by the illusion, $\tau_g(\omega) \propto 2^{-\omega}$ would be required for each allpass section. This can be approximated by setting a to a moderate negative value, for example $a = -0.5$, as shown in Figure 13. A better fit could be produced by optimizing the individual coefficients of the first-order allpass filters, or by applying a more generalized method of fitting the desired group-delay curve [38].

The output of this system when used to process an input of white noise is shown in Figure 14. Note that there are still 16 notches, as in Figure 11. Compared to the version of the system with linearly spaced notches, this system produces a much more convincing Shepard-Risset glissando effect. Some cyclical-sounding behaviour is audible in the very low frequencies, which can be explained by the flattening of the group-delay curve in this region (see Figure 13).

5. CONCLUSIONS

This paper has discussed three different ways to implement infinite phaser and flanging effects, which are called barberpole effects. These effects can be implemented in real time and incorporated as parts of an audio processing environment.

The first proposed method can be interpreted as an inverted version of the Shepard-Risset auditory illusion. Instead of producing an infinitely sweeping tone, it produces infinitely one-way sweeping notches using time-varying notch filters. This processing technique can be used as a digital audio effect for rich-sounding audio material, such as noisy sounds, drums loops, or distorted guitars, to replace the traditional back-and-forth-going phaser.

The second method is a novel dual flanger structure, which is based on a pair of cascaded feedforward comb filters with synchronized modulation controls. Sawtooth waveforms are used to control the length of the delay lines, making the displacement of notches unidirectional. The LFOs used to modulate the second delay line and its gain are in a 90° phase shift in relation to those of

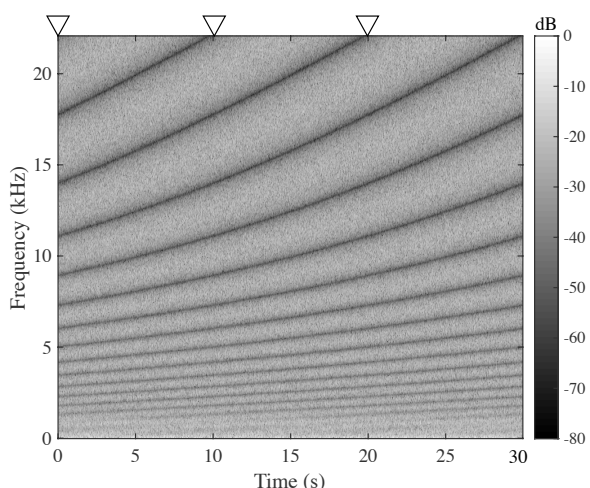


Figure 14: Spectrogram of white noise processed by the structure given in Figure 12. The number of cascaded allpass filters is $D = 32$, the allpass coefficient $a = -0.5$, and the amount of frequency shift is 0.1 Hz.

the first delay line. This results in a smooth cross-fading between delay lines, minimizing the audibility of any abrupt changes in delay lengths. This extension can be called a barberpole flanging effect.

The third method is a digital version of the first barberpole-like phasing effects described by Harald Bode, with a modification proposed to make the notches more closely fit the distribution of tones in a Shepard-Risset illusion. As with the other methods, the effect sounds best with low modulation speeds and with rich spectral content as the input.

In general terms, there are very subtle differences between the proposed techniques. The three of them effectively recreate the illusion of endlessly moving notches. The cyclic nature of the effect is perhaps best hidden in the first implementation, where the notches on the low and high ends of the spectrum are not as audible as those in the middle region. However, this technique is severely restricted to signals with a quasi-flat spectrum. The other proposed techniques are far more versatile, they are not as restricted to a certain type of input. Additionally, their implementation is considerably more economic. For instance, the dual flanger approach can implement a high number of notches without increased complexity. Overall, the biggest limitation of the dual flanger and SSB-modulation methods comes from the fact that, if not properly tuned, their cyclic nature can be easily given away. Audio examples related to all three techniques described in this paper are available at the accompanying website <http://research.spa.aalto.fi/publications/papers/dafx15-barberpole>.

6. ACKNOWLEDGMENTS

The authors would like to thank Dr. Stefan Bilbao and Dr. José Antonio Belloch for their helpful comments during the elaboration of this paper.

7. REFERENCES

- [1] R. N. Shepard, "Circularity in judgments of relative pitch," *J. Acoust. Soc. Amer.*, vol. 36, no. 12, pp. 2346–2353, Dec. 1964.
- [2] R. N. Shepard, "Demonstrations of circular components of pitch," *J. Audio Eng. Soc.*, vol. 31, no. 9, pp. 641–649, Sept. 1983.
- [3] J.-C. Risset, "Pitch control and pitch paradoxes demonstrated with computer-synthesized sounds (abstract)," in *77th Meeting of the Acoustical Society of America*, 1969.
- [4] J.-C. Risset, *Current Directions in Computer Music Research*, chapter 'Paradoxical sounds', pp. 149–158, M. V. Mathews and J. R. Pierce (eds.), The MIT Press, Cambridge, MA, 1989.
- [5] D. Deutsch, "Auditory illusions, handedness, and the spatial environment," *J. Audio Eng. Soc.*, vol. 31, no. 9, pp. 607–618, Sept. 1983.
- [6] D. Stowell, "Scheduling and composing with Risset eternal accelerando rhythms," in *Proc. Int. Computer Music Conf.*, Huddersfield, UK, July 2011.
- [7] B. Bartlett, "A scientific explanation of phasing (flanging)," *J. Audio Eng. Soc.*, vol. 18, no. 6, pp. 674–675, Dec. 1970.
- [8] W. M. Hartmann, "Flanging and phasers," *J. Audio Eng. Soc.*, vol. 26, no. 6, pp. 439–443, Jun. 1978.
- [9] J. O. Smith, *Physical Audio Signal Processing*, W3K Publishing, 2010, online book. See subsection 'Flanging'.
- [10] J. D. Reiss and A. P. McPherson, *Audio Effects: Theory, Implementation and Application*, CRC Press, 2015, See Ch. 2 'Delay Line Effects'.
- [11] M. M. Wanderley and P. Depalle, "Gesturally controlled digital audio effects," in *Proc. COST-G6 Conf. Digital Audio Effects (DAFx-01)*, Limerick, Ireland, Dec. 2001, pp. 165–169.
- [12] M. M. Wanderley and P. Depalle, "Gestural control of sound synthesis," *Proceedings of the IEEE*, vol. 92, no. 4, pp. 632–644, Apr. 2004.
- [13] M. L. Beigel, "A digital "phase shifter" for musical applications, using the Bell Labs (Alles-Fischer) digital filter module," *J. Audio Eng. Soc.*, vol. 27, no. 9, pp. 673–676, Sept. 1979.
- [14] J. O. Smith, "An allpass approach to digital phasing and flanging," in *Proc. Int. Computer Music Conf.*, Paris, France, Oct. 1984, pp. 103–109.
- [15] V. Välimäki, S. Bilbao, J. O. Smith, J. S. Abel, J. Pakarinen, and D. Berners, "Virtual analog effects," in *DAFX: Digital Audio Effects*, U. Zölzer, Ed., pp. 473–522. Wiley, Chichester, UK, second edition, 2011.
- [16] H. Bode, "History of electronic sound modification," *J. Audio Eng. Soc.*, vol. 32, no. 10, pp. 730–739, Oct. 1984.
- [17] O. Larkin, "Endless Series," Software and sound examples available at <http://www.olilarkin.co.uk/index.php?p=eseries>, accessed June 4, 2015.
- [18] C. Budde, "Barberpole Flanger," VST effect plug-in for Windows available at http://www.kvraudio.com/product/barberpole_flanger_by_christian_budde, accessed June 4, 2015.

- [19] A. Huovilainen, “Enhanced digital models for analog modulation effects,” in *Proc. Int. Conf. Digital Audio Effects (DAFx-05)*, Madrid, Spain, Sept. 2005, pp. 155–160.
- [20] C. Raffel and J. Smith, “Practical modeling of bucket-brigade device circuits,” in *Proc. Int. Conf. Digital Audio Effects (DAFx-10)*, Graz, Austria, Sept. 2010.
- [21] F. Eichas, M. Fink, M. Holters, and U. Zölzer, “Physical modeling of the MXR Phase 90 guitar effect pedal,” in *Proc. Int. Conf. Digital Audio Effects (DAFx-14)*, Erlangen, Germany, Sept. 2014, pp. 153–166.
- [22] T. Wilmering, G. Fazekas, and M. B. Sandler, “Audio effect classification based on auditory perceptual attributes,” in *Proc. AES 135th Convention*, New York, USA, Oct. 2013.
- [23] M. Stein, J. Abeßer, C. Dittmar, and G. Schuller, “Automatic detection of audio effects in guitar and bass recordings,” in *Proc. AES 128th Convention*, London, UK, May 2010.
- [24] S. J. Orfanidis, *Introduction to Signal Processing*, chapter ‘IIR Digital Filter Design’, Prentice Hall International Editions, Englewood Cliffs, NJ, USA, 1996.
- [25] V. Välimäki and T. I. Laakso, “Suppression of transients in variable recursive digital filters with a novel and efficient cancellation method,” *IEEE Trans. Signal Process.*, vol. 46, no. 12, pp. 3408–3414, Dec. 1998.
- [26] V. Välimäki, “Discrete-time synthesis of the sawtooth waveform with reduced aliasing,” *IEEE Signal Process. Lett.*, vol. 12, no. 3, pp. 214–217, Mar. 2005.
- [27] H.-M. Lehtonen, V. Välimäki, and T. I. Laakso, “Canceling and selecting partials from musical tones using fractional-delay filters,” *Comp. Music J.*, vol. 32, no. 2, pp. 43–56, Summer 2008.
- [28] T. I. Laakso, V. Välimäki, M. Karjalainen, and U. K. Laine, “Splitting the unit delay—Tools for fractional delay filter design,” *IEEE Signal Process. Mag.*, vol. 13, no. 1, pp. 30–60, Jan. 1996.
- [29] D.E. Norgaard, “The phase-shift method of single-sideband signal generation,” *Proc. of the IRE*, vol. 44, no. 12, pp. 1718–1735, Dec 1956.
- [30] L. R. Rabiner and R. W. Schafer, “On the behavior of minimax FIR digital Hilbert transformers,” *Bell Syst. Tech. J.*, vol. 53, no. 2, pp. 363–390, 1974.
- [31] S. Disch and U. Zölzer, “Modulation and delay line based digital audio effects,” in *Proc. Second COST G-6 Workshop on Digital Audio Effects (DAFx-99)*, Trondheim, Norway, Dec. 1999, pp. 5–8.
- [32] S. Wardle, “A Hilbert-transformer frequency shifter for audio,” in *Proc. First COST G-6 Workshop on Digital Audio Effects (DAFx-98)*, Barcelona, Spain, Nov. 1998, pp. 25–29.
- [33] R. Ansari, “IIR discrete-time Hilbert transformers,” *IEEE Trans. Acoustics, Speech, Signal Process.*, vol. 35, no. 8, pp. 1116–1119, Aug. 1987.
- [34] V. Välimäki, J. S. Abel, and J. O. Smith, “Spectral delay filters,” *J. Audio Eng. Soc.*, vol. 57, no. 7–8, pp. 521–531, Jul. 2009.
- [35] V. Välimäki, J. Parker, and J. S. Abel, “Parametric spring reverberation effect,” *J. Audio Eng. Soc.*, vol. 58, no. 7–8, pp. 547–562, Jul. 2010.
- [36] J. Parker, “Efficient dispersion generation structures for spring reverb emulation,” *EURASIP J. Advances in Signal Processing*, vol. 2011, no. 646134, pp. 521–531, Mar. 2011.
- [37] J. Pekonen, T. Pihlajamäki, and V. Välimäki, “Computationally efficient Hammond organ synthesis,” in *Proc. Int. Conf. Digital Audio Effects (DAFx-11)*, Paris, France, Sept. 2011, pp. 19–22.
- [38] J. S. Abel and J. O. Smith, “Robust design of very high-order allpass dispersion filters,” in *Proc. 9th Int. Conf. Digital Audio Effects (DAFx-06)*, Montreal, Canada, Sept. 2006, pp. 13–18.